Numerical study of supercritical airfoil with integrated impeller power plant

© E.A. Pigusov, A.I. Volkov, M.V. Dolotin, S.A. Kuzin

Zhukovsky Central Aerohydrodynamic Institute, Zhukovsky, Moscow oblast, Russia
E-mail: sergey.kuzin.1994@mail.ru

Received May 5, 2025
Revised August 18, 2025
Accepted August 19, 2025

Numerical study results of the supercritical airfoil equipped with adaptive multi-segment moving flap with integrated impeller power plant are presented. Two types of the leading-edge devices are considered: the droop nose and bull-nose Krueger flap. The lift coefficient dependence on the angle of attack is obtained. An influence of the both leading-edge type and leading-edge deflection angle on the lift is shown. The main flow features on take-off and landing modes are revealed.

Keywords: supercritical airfoil, distributed impeller power plant, adaptive flap, leading-edge devices, lift efficiency.

DOI: 10.61011/TPL.2025.12.62800.8085

Developing the design of next-generation regional aircraft, one needs to take into account the requirement of suitability for short runways combined with a high cruising speed and satisfactory fuel efficiency. These conflicting requirements may be satisfied through the use of powered lift systems (PLSs) [1,2]. With recent advances in electric propulsion technology, a distributed impeller power plant (DIPP) integrated with the lifting surfaces may be regarded as a

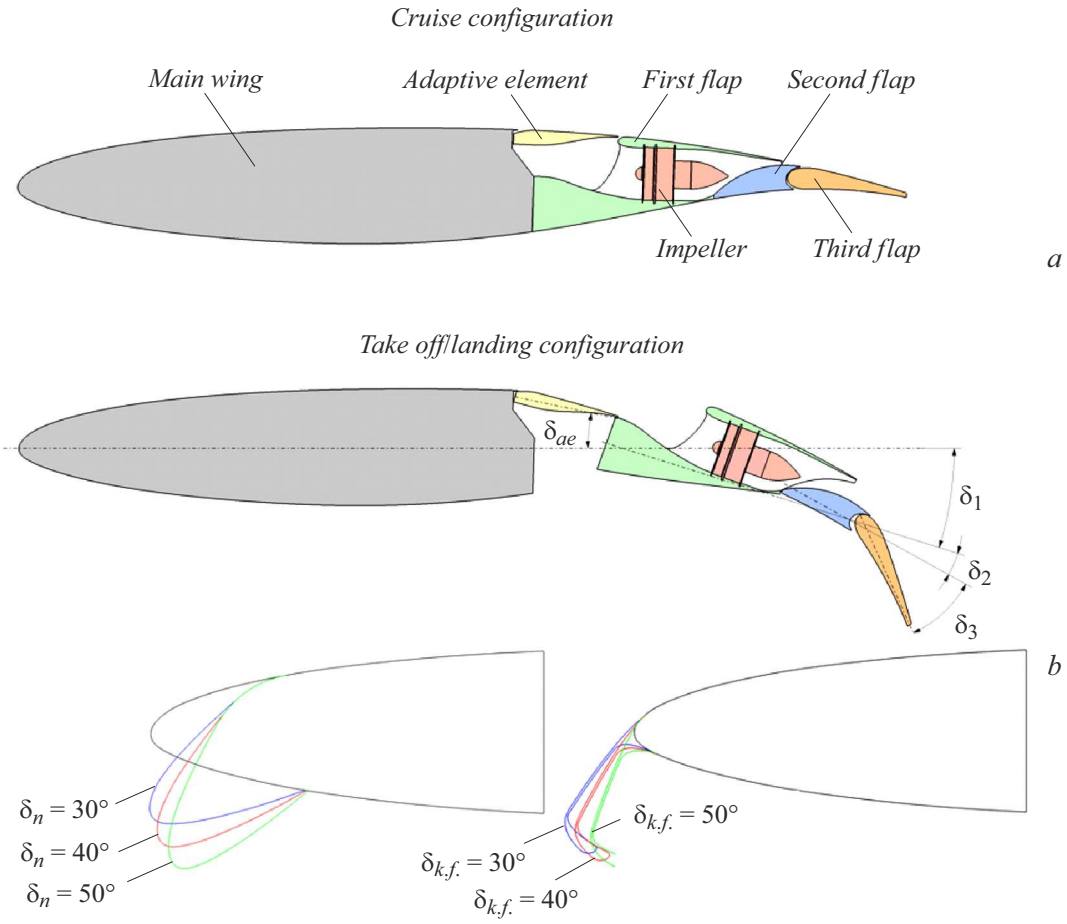

Figure 1. Object of study. *a* — Cruising and take-off/landing configurations; *b* — deflection angles of leading-edge devices.

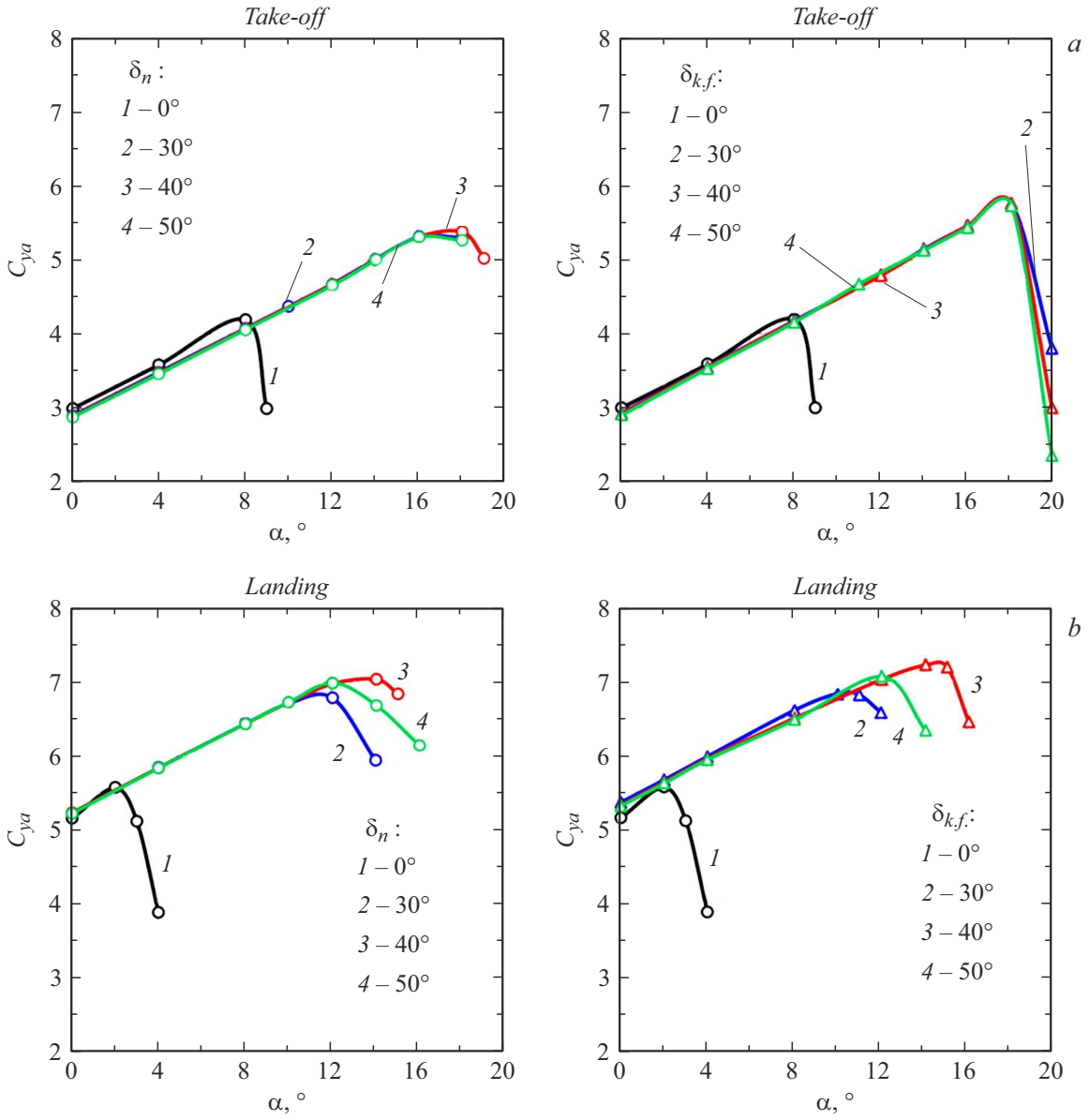

Figure 2. Dependences $C_{ya}(\alpha)$ at different leading-edge device deflection angles. *a* — Take-off configuration; *b*— landing configuration.

promising PLS option. This engineering solution allows one to raise significantly the lift coefficient and reduce the characteristic flight speeds in take-off and landing modes [3,4].

Swept supercritical airfoil designs are used to ensure high cruising speeds of passenger aircraft [5]. Such airfoils provide an opportunity to increase the critical Mach number of incident flow at which a significant wave aerodynamic drag arises. Supercritical airfoils have a small leading edge radius, which may result in early separation of the boundary layer in take-off and landing modes due to the emergence of an unfavorable pressure gradient at the leading edge (especially in those cases where a DIPP is used). This necessitates the use of leading-edge devices to increase the critical angle of attack.

In the present paper, we report the results of computational studies of a section of an infinite-span supercritical airfoil with an adaptive element, which may also operate in the interceptor mode, and a three-link retractable flap with an integrated DIPP (Fig. 1, *a*) with an impeller fan diameter of 140 mm. Two types of leading-edge devices were considered: a droop nose and a bull-nose Krueger flap. Calculations were performed with the trailing-edge devices in take-off and landing positions. In the take-off configuration, the deflection angle of the adaptive element was $\delta_{ae} = 12°$, and the deflection angles of links were $\delta_1 = 5°$, $\delta_2 = 17°$, and $\delta_3 = 0°$, respectively. In the landing configuration, the deflection angle of the adaptive element remained unchanged, and the deflection angles of links were $\delta_1 = 18°$, $\delta_2 = 17°$, and $\delta_3 = 11°$, respectively.

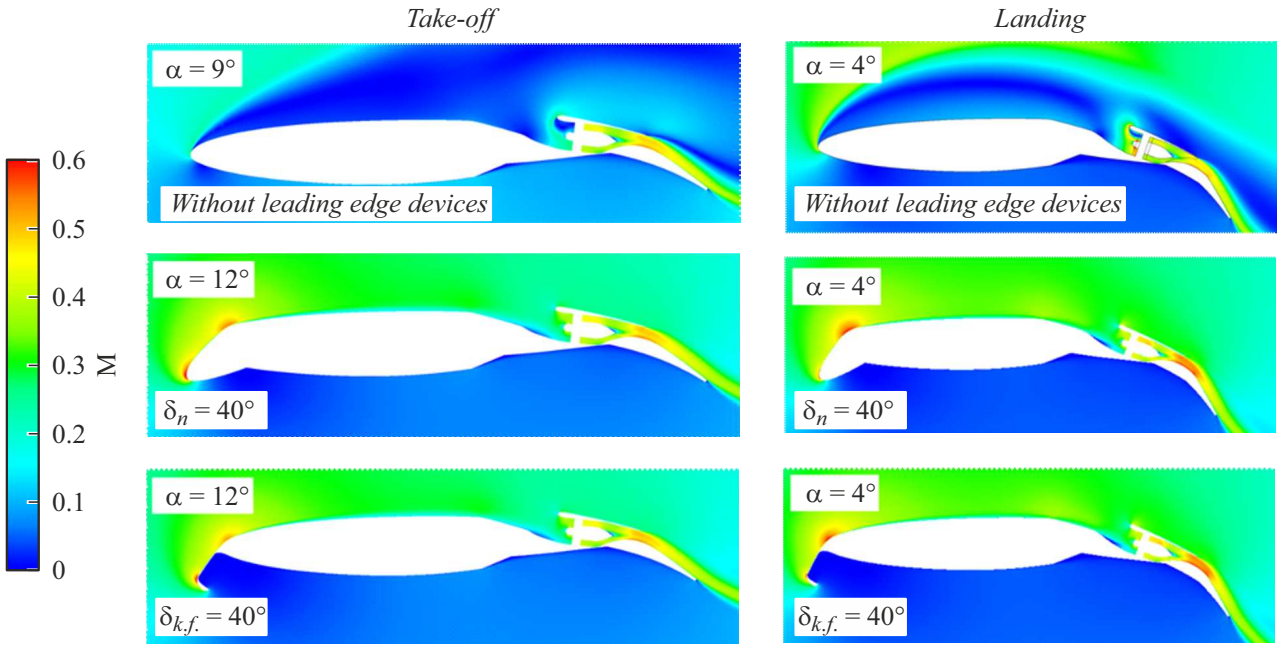

Figure 3. Mach number distribution patterns for take-off and landing configurations and various leading-edge device designs.

Various deflection angles of leading-edge devices were examined in these configurations. The deflection angle of the droop nose was $\delta_n = 30°/40°/50°$; the bull-nose Krueger flap was deflected to positions where its leading edge coincided with the leading edge of the droop nose (for convenience, the corresponding deflection angles are denoted as $\delta_{k.f.} = 30°/40°/50°$) (Fig. 1, *b*). Calculations were performed for incident flow conditions corresponding to $H = 0$ km (ISA), Mach number $\mathrm{M} = 0.15$, and Reynolds number $\mathrm{Re} = 8.2 \cdot 10^6$. The power supplied to each impeller was $N_{imp} = 20$ kW, which is fairly high for electric motors of this size. The angle of attack varied within the range from 0° to beyond-stall values. Airfoil chord $b = 2.4$ m was set as the characteristic dimension for determining the aerodynamic force coefficients.

Computational domains in the form of $64 \times 64 \times 0.32$ m rectangular parallelepipeds were prepared for computational studies. Finite-volume unstructured tetrahedral computational grids with $\sim 2.2 \cdot 10^7$ elements were formed in these domains. Prismatic layers ($\sim 1.1 \cdot 10^7$ cells) with the height of the first cell providing an average value of $y^+ < 1$ were used to resolve the boundary layer flow.

Calculation studies were carried out by solving the Reynolds-averaged Navier–Stokes equations numerically. The SST (shear stress transport) turbulence model was used to close the Navier–Stokes equations. The DIPP was simulated using the „active disk“ method in a way similar to how it was done in [3,4,6]: relative static pressure and total temperature with constant distributions over the area were specified at the fan „inlet“ boundary, and relative total pressure and total temperature with constant distributions over the area were specified at the straightener „outlet“ boundary. The consistency of air flow through the „inlet“ and „outlet“ boundaries and the correspondence of boundary conditions of the power supply to the impeller motor was maintained using the equations of one-dimensional gas dynamics [7,8].

Figures 2, *a* and *b* present the dependences of lift coefficient C_{ya} on angle of attack α for take-off and landing configurations with different deflection angles of leading-edge devices. The results of calculation studies reveal that the angle of attack at which the maximum lift is achieved is $\alpha_{Cya\,\max} = 8°$ in the take-off configuration with non-deflected leading-edge devices. With the droop nose deflected, the maximum C_{ya} is reached at $\delta_n = 40°$ and $\alpha = 18°$. Dependences $C_{ya}(\alpha)$ for airfoils with deflected bull-nose Krueger flaps remain virtually unchanged throughout the entire range of angles of attack up to $\alpha = 18°$, where $C_{ya\,\max}$ is reached at all deflection angles. In the landing configuration with non-deflected leading-edge devices, $\alpha_{Cya\,\max} = 2°$. Among all the considered angles of deflection of the droop nose and the bull-nose Krueger flap, the maximum $C_{ya\,\max}$ values in the landing configuration are achieved at $\delta_n = 40°$ and $\delta_{k.f.} = 40°$ (the corresponding $\alpha_{Cya\,\max} = 14°$). The calculated dependences demonstrate that a $\delta_{k.f.} = 40°$ deflection of the bull-nose Krueger flap provides a 7.2 % (in the take-off configuration) or 2.6 % (in the landing configuration) $C_{ya\,\max}$ increase relative to $C_{ya\,\max}$ obtained with the deflected droop nose.

In take-off configurations, the flow patterns at zero angle of attack and all leading-edge device deflection angles are similar; the difference is in the separated flow behind the bull-nose Krueger flap. In the landing configuration without leading-edge devices and zero angle of attack, an

attached separation flow is observed, which is eliminated when leading-edge devices are deflected.

A comparison of the flow patterns for airfoils without leading-edge devices at beyond-stall angles of attack with the flow around airfoils with leading-edge devices at close angles of attack (Fig. 3) reveals a large separation region in the design without leading-edge devices, which vanishes when leading-edge devices are introduced.

Comparing the Mach number distributions for airfoils with leading-edge devices at $\delta_n = 40^\circ$ and $\delta_{k.f.} = 40^\circ$ and angles of attack $\alpha_{C_{ya}\max}$, one may note an attached separation flow in the distribution corresponding to the design with the droop nose in the take-off configuration. This flow feature is the reason why $C_{ya\max}$ decreases relative to the case of bull-nose Krueger flap deflection. In the landing configuration at $\alpha_{C_{ya}\max}$, the designs with the droop nose and bull-nose Krueger flap do not feature any apparent separation flow on the upper surface. Since the flow patterns differ only slightly, the $C_{ya\max}$ values are close (the difference is 2.6%). With a further increase in angle of attack, a developed separation flow forms in the landing configuration with the deflected droop nose and bull-nose Krueger flap.

Thus, the leading-edge device providing the highest efficiency in the take-off and landing configurations of the object under study is the bull-nose Krueger flap with deflection angle $\delta_{k.f.} = 40^\circ$ in both configurations. It should be noted that the rational angle of deflection of the Krueger flap may change with a change in the DIPP operating mode due to a possible shift of the stagnation point of incident flow.

Conflict of interest

The authors declare that they have no conflict of interest.

References

[1] A.V Petrov, *Energeticheskie metody uvelicheniya pod"emnoi sily kryla* (Fizmatlit, M., 2011) (in Russian).
[2] A.V. Petrov, *Aerodinamika transportnykh samoletov korotkogo vzleta i posadki s energeticheskimi sistemami uvelicheniya pod"emnoi sily* (Innovatsionnoe Mashinostr., M., 2018) (in Russian).
[3] A.I. Volkov, M.V. Dolotin, V.G. Kazhan, S.A. Kuzin, E.A. Pigusov, Uch. Zap. Tsentr. Aerogidrodin. Inst., **54** (6), 12 (2023) (in Russian).
[4] A.I. Volkov, M.V. Dolotin, S.A. Kuzin, E.A. Pigusov, Uch. Zap. Tsentr. Aerogidrodin. Inst., **50** (6), 30 (2024) (in Russian).
[5] J.D. Anderson, *Fundamentals of aerodynamics* (McGraw–Hill Education, N.Y., 2017), p. 775–777.
[6] M. Trancossi, M. Madonia, *The efficiency of an electric turbofan vs. inlet area: A simple mathematical model and CFD simulations*, SAE technical paper 2012-01-2217 (2012). DOI: 10.4271/2012-01-2217
[7] L.G. Loitsyanskii, *Mekhanika zhidkosti i gaza* (Nauka, M., 1987) (in Russian).
[8] G.N. Abramovich, *Prikladnaya gazovaya dinamika* (Nauka, M., 1991) (in Russian).

Translated by D.Safin